RESEARCH ARTICLE OPEN ACCESS

# Photocatalytic Studies of Anatase and Rutile phase $TiO_2$ Nanocrystals Prepared via Solvothermal method

S.Perumal
(Principal, S. T. Hindu College, Nagercoil-2)

**Abstract**
Nanocrystals of $TiO_2$ photocatalyst have been synthesized by solvothermal method. The photocatalysts were characterized by XRD, UV–Vis spectroscopy and photocatalytic study. The analysis from X-ray diffraction revealed that the annealed product at 1000˚C shows crystal phase of rutile and all others are in anatase phase. FTIR spectra show the vibration of Ti-O bands around 650 $cm^{-1}$. UV-Vis spectra indicated the band gap value of annealed samples.

***Key Words*** – Calcination, Nanocrystals, Photocatalysis, Solvothermal, $TiO_2$

## I. INTRODUCTION

$TiO_2$ is known as an effective photocatalyst because of its purification efficiency of water and air. The photocatalytic efficiency of $TiO_2$ depends on many factors, such as crystalline phase, particle size and surface area[1]. $TiO_2$ exists in three phases. They are anatase, brookite and rutile. Anatase and brookite are transformed to rutile phase at higher temperatures. Anatase phase has more surface energy than rutile. So it is more applicable in photocatalysis [2]. The band gap value of $TiO_2$ is 3.2 eV. The wavelength range of UV light is in this band gap (<387 nm) region, which means to get enhanced photocatalytic activity, we should excite the $TiO_2$ nanocrystals by UV light. To get visible light active $TiO_2$ nanocrystals modify the band gap in the visible region [3]. In this present study $TiO_2$ nanocrystals are prepared by solvothermal method and annealed to three different temperatures. The photocatalytic activities of the prepared and annealed samples under UV irradiation are reported here.

## II. EXPERIMENTAL

### 2.1 Materials

Titanium tetra-isopropoxide (TTIP, 97%, Sigma Aldrich), Toluene (99.8%, HPLC).

### 2.2 Preparation of Nanocrystals

All reagents were used without further purification process. 0.5 M of TTIP was mixed with 100 ml toluene in Teflon lined stainless steel autoclave without stirring (200 ml capacity, 80% filling). Then it was heated to 250˚C with a rate of 5˚ C/min and maintained up to five hours in an oven. After cooling gradually to room temperature, the obtained precipitate was separated with centrifugal separator and then dried in vacuum. The collected products were annealed to three various temperatures about 600˚C, 800˚C and 1000˚C. They are named as $TiO_2$-600, $TiO_2$-800 and $TiO_2$-1000.

## III. CHARACTERIZATION

The Powder X-ray diffraction data of $TiO_2$ nanocrystals were characterized by using XPERTPRO diffractometer. FTIR spectra of $TiO_2$ nanocrystals were recorded by using Jasco 4100 Spectrophotometer equipped with ATR. The UV-Visible DRS spectra were taken by Shimadzu UV 2600 UV-Visible spectrometer. Photocatalytic measurements were carried out by using Systronics-2201 UV-Visible double beam spectrophotometer.

## IV. RESULTS AND DISCUSSION

### 4.1 Powder X-ray diffraction analysis

Fig. (1) Shows the powder X-ray diffraction data of prepared and calcinated $TiO_2$ nanocrystals. The intensity of the peaks increases with increasing calcinating temperature and the width of the (101) plane diffraction peak of anatase becomes narrower [4]. The strong and sharp peaks indicate the formation of larger crystal sizes and higher degrees of crystallinity [5]. The powder X-ray diffraction data of prepared $TiO_2$, $TiO_2$-600 and $TiO_2$-800 are in good agreement with standard JCPDS (JDPDS 21-1272) of an anatase crystalline phase of $TiO_2$. The powder X-ray diffraction data of $TiO_2$-1000 is in good agreement with standard JCPDS (JDPDS 21-1276) of rutile crystalline phase of $TiO_2$. The calculated lattice parameter values are shown in Table (1).

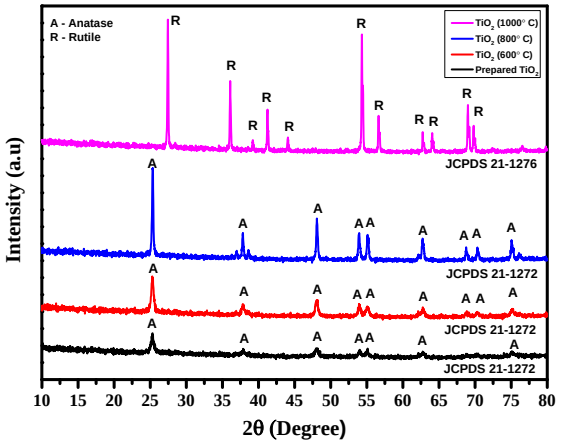


**Fig 1. Powder X-ray diffraction data of prepared and calcinated $TiO_2$ nanocrystals**

The crystallite size of $TiO_2$ nanocrystals were calculated by Scherrer equation, $D=K \lambda / \beta \cos \theta$, where D is the crystallite size, λ is the wavelength of X-ray radiation (Cu Kα-1radiation= 1.54060 Å), K is a constant and usually taken as 0.9, β is the full width at half maximum (FWHM) after subtraction of equipment broadening, and θ is the half of the Bragg angle [6]. For crystallite size calculation (1 0 1) plane of the anatase phase and (1 1 0) plane of the rutile phase was considered.

**Table 1: Lattice parameters for prepared and calcinated $TiO_2$ nanocrystals**

| Sample Name | Prepared $TiO_2$ | $TiO_2$-600 | $TiO_2$-800 | $TiO_2$-1000 |
|---|---|---|---|---|
| Crystal structure | Tetragonal | Tetragonal | Tetragonal | Tetragonal |
| a | 3.78382 | 3.78477 | 3.78598 | 4.59484 |
| b | 3.78382 | 3.78477 | 3.78598 | 4.59484 |
| c | 9.50549 | 9.50886 | 9.51365 | 2.96129 |
| Volume (Å)$^3$ | 136.093 | 136.210 | 136.365 | 62.521 |
| Crystallite size (nm) | 40 | 30 | 60 | 70 |

### 4.2 FTIR analysis

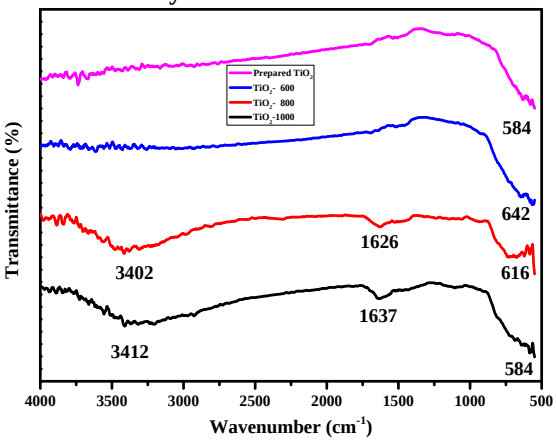


**Fig 2. FTIR spectra of prepared and calcinated $TiO_2$ nanocrystals**

Fig. (2) Shows FTIR spectra of prepared and calcinated $TiO_2$ crystals. Prepared $TiO_2$ and $TiO_2$-600 show surface adsorbed stretching O-H vibration of molecular water at 3412 $cm^{-1}$ and 3402 $cm^{-1}$ respectively. Similarly, the bending O-H vibration of molecular water was observed at 1637$cm^{-1}$ and 1626 $cm^{-1}$ respectively[7]. At this ranges no vibrational peak was observed at higher calcinating temperature nano crystal of $TiO_2$-800 and $TiO_2$-1000. This is due to the removal surface adsorbed molecular water at higher calcinating temperatures. The peaks at 587, 621 and 627 $cm^{-1}$ were assigned to Ti-O vibration mode of anatase phase (Prepared $TiO_2$, $TiO_2$-600 and $TiO_2$-800). The rutile phase ($TiO_2$-1000) Ti-O vibration mode was observed at 633 $cm^{-1}$[8].

### 4.3 UV-Vis spectral analysis

The optical band gap value of the prepared and calcinated $TiO_2$ nano crystals were found out using diffuse reflectance spectra. The diffuse reflectance data were transformed to absorption data using Kubelka-Munk formula, $F(R) = (1-R)^2/2R$, where reflectance, $R = R_{sample} / R_{reference}$[9]. F(R) is Kubelka-Munk function which corresponds to the linear absorbance coefficient α. The relation between the absorption coefficient a and the incident photon energy hy is defined by the following relation,

$$(\alpha h\nu) = B\,(h\nu - E_g)^n$$

where $E_g$ is the optical band gap, B is a constant, hν is the photon energy and n is the index that depends on nature of transition. For indirect transition

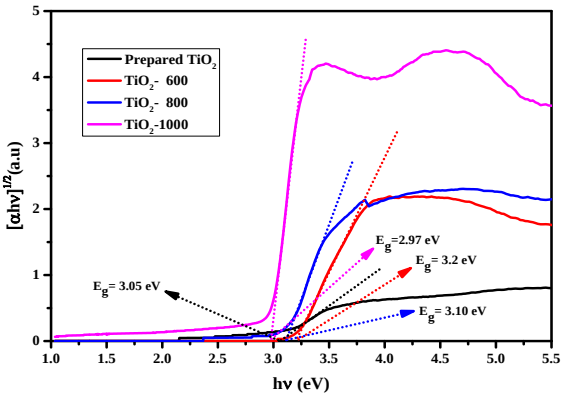


**Fig 3. UV-Vis spectra of prepared and calcinated $TiO_2$ nanocrystals**

n=2[10]. The Kubelka-Munk function allows the construction of a Tauc Plot: $(\alpha h\nu)^{1/2}$ vs hν shown in Fig. (3) [9]. The optical band gap value for prepared $TiO_2$, $TiO_2$-600, $TiO_2$-800 and $TiO_2$-1000 found from the Tauc plot were 3.05, 3.2, 3.10 and 2.97 eV respectively.

### 4.4 Photocatalytic studies

The photocatalytic activity of prepared $TiO_2$, $TiO_2$-600, $TiO_2$-800 and $TiO_2$-1000 were evaluated by examining the degradation of methyl orange under UV light (18 W, UV-A fluorescent lamp) irradiation. For this typical study, 50 ml of 10 ppm aqueous methyl orange solution was taken in a 100 ml beaker. 100 mg of $TiO_2$ nanocrystals, in the form of powder, was dispersed in this solution. The solution was irradiated with UV light up to 210 min. The degradation of methyl orange solution was observed by UV-Vis absorption spectra of methyl orange solution. For this study every half an hour 5 ml of methyl orange solution was taken out and was centrifuged immediately to remove the nano crystal of catalyst $TiO_2$. Fig. (4-7) shows the absorption spectra of methyl orange solution irradiated with UV lamp over prepared $TiO_2$, $TiO_2$-600, $TiO_2$-800 and $TiO_2$-1000.

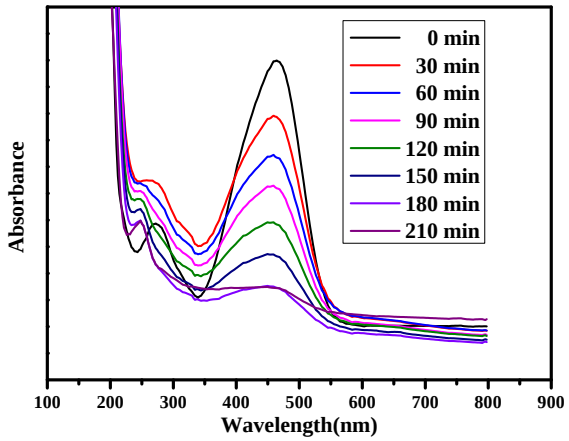


**Fig 4. Photocatalytic absorption spectra of prepared $TiO_2$ nanocrystals**

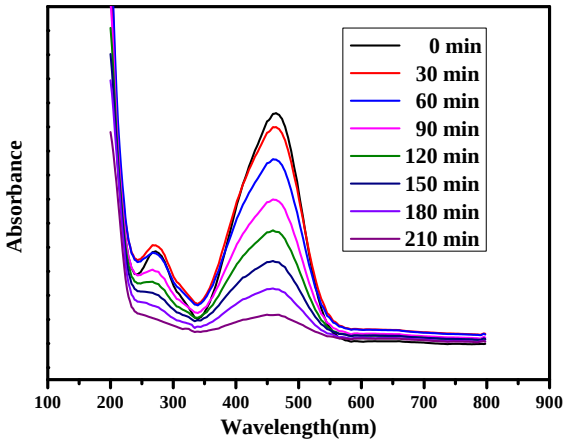


**Fig 5. Photocatalytic absorption spectra of $TiO_2$-600 nanocrystals**

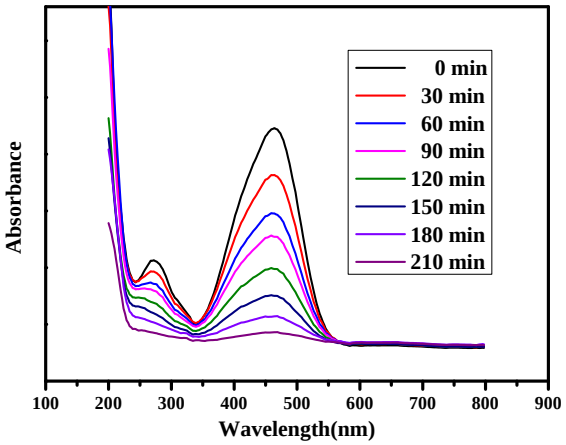


**Fig 6. Photocatalytic absorption spectra of $TiO_2$-800 nanocrystals**

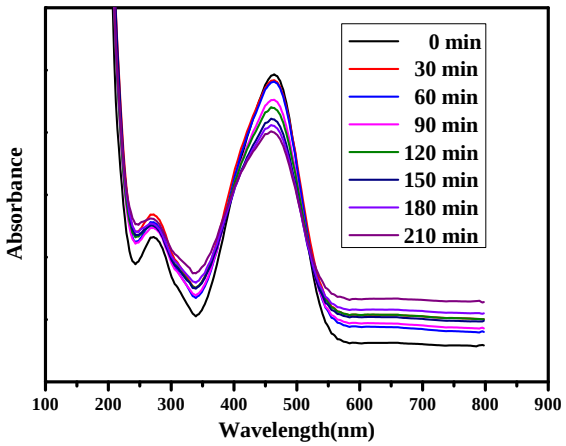


**Fig 7. Photocatalytic absorption spectra of $TiO_2$-1000 nanocrystals**

The degradation efficiency of the prepared $TiO_2$, $TiO_2$-600, $TiO_2$-800 and $TiO_2$-1000 are shown in Fig. (8).

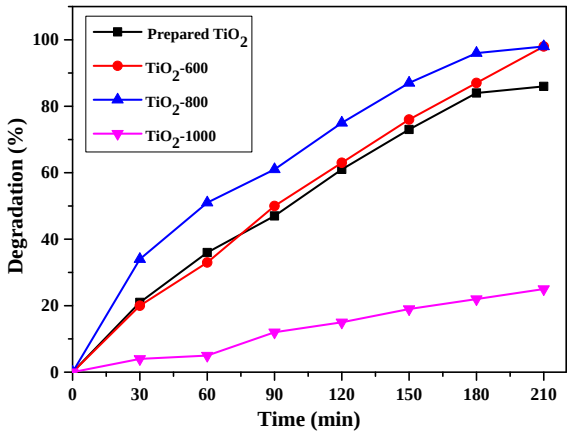


**Fig 8. Degradation efficiency $TiO_2$ nanocrystals**

The prepared $TiO_2$ shows 86% of degradation at the time of 210 min. $TiO_2$-600 and $TiO_2$-800 show the same amount of degradation, 98%. These three nanocrystals are in anatase phase and shows lower crystallite size. The UV-Vis spectral study also confirms that the band gap values are in UV radiation excitation range. So the degradation value is high under UV irradiation. $TiO_2$-1000 shows the lowest value of degradation of 25%. This is due to increase in crystallite size by calcinations. Further UV data confirms that the band edge shifted to visible region decrease the excitation of $TiO_2$ nano crystals in rutile phase. So the degradation is very low when compared to anatase phase $TiO_2$-600 and $TiO_2$-800 under UV irradiation [11].

## V. CONCLUSIONS

In this study, $TiO_2$ nanocrystals were successfully synthesized by solvothermal method and its photocatalytic activity was tested in degradation of methyl orange model pollutant. X-ray diffraction result shows the increase in crystalline size with increase in calcination temperatures. These results suggest that the photocatalytic activity strongly depends on size and phase of the crystalline. The anatase phase prepared $TiO_2$, $TiO_2$-600 and $TiO_2$-800 nanocrystals show higher photocatalytic activity than rutile phase $TiO_2$-1000.

## VI. ACKNOWLEDGEMENTS

I acknowledge University Grants Commission, New Delhi, for financial support through a Major Project.

## REFERENCES

[1]. G. Liu, S. Chen, Q. L. Haibin Li, Novel Fe doped mesoporous $TiO_2$ microspheres:Ultrasonic–hydrothermal synthesis, Characterization, and photocatalytic properties, *Physica E, 42*, 2010, 1844–1849.

[2]. S. Tian, H. Zhao, R. Jin,Y. Chen, B. Liu, H. Yang M. Cui, Solvothermal synthesis and enhanced photocatalytic activity of flower like nanoarchitectures assembled from anatase $TiO_2$ nanoflakes, *Physica E, 44*, 2012. 2110–2117.

[3]. T. He, X. Zhang J. Cui, Synthesis of $Fe_3O_4$@$SiO_2$@Pt ion–$TiO_2$ hybrid composites with high efficient UV–visible light photoactivity, *Catalysis Communications, 40*, 2013,. 66–70

[4]. J. Yu, W. Ho, Z. Jiang, L. Zhang J.C. Yu, Effects of F- Doping on the Photocatalytic Activity and Microstructures of Nanocrystalline $TiO_2$ Powders, *Chemistry of Materials*, 2002, 3808-3816.

[5]. J.-Y. Park, J.-W. Lee D.-Y. Choi, Adsorption and photocatalysis of spherical $TiO_2$ particles prepared by hydrothermal reaction, *Materials Letters*, *89*, 2012, 212–215.

[6]. H. Eskandarloo, N. Modirshahla, M. Shokri, M.A. Behnajady, Investigation of the effect of sol–gel synthesis variables on structural and photocatalytic properties of $TiO_2$ nanoparticles, *Desalination, 278*, 2011, 10–17.

[7]. J. C. Yu, L. Wu, L. Zhang, J. Yu, X. Wang, Characterization of mesoporous nanocrystalline $TiO_2$ photocatalysts synthesized via a sol-solvothermal process at a low temperature, *Journal of Solid State Chemistry, 178*, 2005, 321–328.

[8]. Y. Mo, B. Zheng, H.Yuan, D. Xiao, J. Nie, Electrochemical fabrication of lanthanum-doped $TiO_2$ nanotube array electrode and investigation of its photoelectrochemical capability, *Electrochimica Acta, 90*, 2013, 589– 596.

[9]. W. Rui, M. Krause, B. B. Mamba Alex T. Kuvarega, Nitrogen/Palladium-Codoped $TiO_2$ for Efficient Visible Light Photocatalytic Dye Degradation, *Journal of Physical Chemistry C, 115*, 2011, 22110–22120.

[10]. F. Yakuphanoglu, Semiconducting and quartz microbalance (QCM) humidity sensor properties of $TiO_2$ by sol gel calcination method, *Solid State Sciences*, *14*, 2012, 673-676.

[11]. H. Eskandarloo, N. Modirshahla, M. Shokri, M.A. Behnajady, Investigation of the effect of sol–gel synthesis variables on structural and photocatalytic properties of $TiO_2$ nanoparticles, *Desalination, 278*, 2011, 10–17.